Earth Surface Processes and Landforms
Earth Surf. Process. Landforms **32**, 2019–2037 (2007)
Published online 17 April 2007 in Wiley InterScience
(www.interscience.wiley.com) **DOI:** 10.1002/esp.1513

The influence of riparian vegetation on near-bank turbulence: a flume experiment

Maeve McBride,[1]* W. Cully Hession,[2] Donna M. Rizzo[1] and Douglas M. Thompson[3]
[1] *Civil and Environmental Engineering, University of Vermont, Burlington, VT, USA*
[2] *Biological Systems Engineering, Virginia Tech, Blacksburg, VA, USA*
[3] *Department of Physics, Astronomy, and Geophysics, Connecticut College, New London, CT, USA*

**Correspondence to: Maeve McBride, Civil and Environmental Engineering, University of Vermont, 213 Votey Building, Burlington, VT 05405, USA. E-mail: mmcbride@cems.uvm.edu*

Received 11 March 2006; Revised 25 January 2007; Accepted 12 February 2007

Abstract

Measurements from a fixed-bed, Froude-scaled hydraulic model of a stream in northeastern Vermont demonstrate the importance of forested riparian vegetation effects on near-bank turbulence during overbank flows. Sections of the prototype stream, a tributary to Sleepers River, have increased in channel width within the last 40 years in response to passive reforestation of its riparian zone. Previous research found that reaches of small streams with forested riparian zones are commonly wider than adjacent reaches with non-forested, or grassy, vegetation; however, driving mechanisms for this morphologic difference are not fully explained. Flume experiments were performed with a 1:5 scale, simplified model of half a channel and its floodplain, mimicking the typical *non-forested* channel size. Two types of riparian vegetation were placed on the constructed floodplain: non-forested, with synthetic grass carpeting; and forested, where rigid, randomly distributed, wooden dowels were added. Three-dimensional velocities were measured with an acoustic Doppler velocimeter at 41 locations within the channel and floodplain at near-bed and 0·6-depth elevations. Observations of velocity components and calculations of turbulent kinetic energy (TKE), Reynolds shear stress and boundary shear stress showed significant differences between forested and non-forested runs. Generally, forested runs exhibited a narrow band of high turbulence between the floodplain and main channel, where TKE was roughly two times greater than TKE in non-forested runs. Compared to non-forested runs, the hydraulic characteristics of forested runs appear to create an environment with higher erosion potential. Given that sediment entrainment and transport can be amplified in flows with high turbulence intensity and given that mature forested stream reaches are wider than comparable non-forested reaches, our results demonstrated a possible driving mechanism for channel widening during overbank flow events in stream reaches with recently reforested riparian zones. Copyright © 2007 John Wiley & Sons, Ltd.

Keywords: bank erosion; channel morphology; riparian vegetation; turbulent kinetic energy; shear stress

Introduction

Reforestation of riparian areas is a common phenomenon due both to restoration efforts and passive reforestation. Stream restoration programs typically include riparian reforestation to benefit stream ecosystems by filtering pollutants, regulating light and temperature regimes, and providing physical habitat and a food/energy base (Gregory *et al.*, 1991; Sweeney, 1992; Sweeney *et al.*, 2004). Some riparian areas have passively reforested in response to changes in land use, especially in areas where agricultural uses are in decline. For example, late nineteenth-century Vermont was roughly 30 per cent forested; however, about 70 per cent of Vermont is currently forested (Albers, 2000). In this study, we used a scaled flume experiment to explore the effects of reforestation on the hydraulic characteristics of overbank flows, a potential driver for morphologic change.

Riparian vegetation exerts a strong influence on stream-channel morphology. Studies from different geographic locations indicate that stream reaches with riparian forests are wider than those with adjacent grassy vegetation (Zimmerman *et al.*, 1967; Murgatroyd and Ternan, 1983; Sweeney, 1992; Davies-Colley, 1997; Trimble, 1997; Hession *et al.*, 2000, 2003; Sweeney *et al.*, 2004; Allmendinger *et al.*, 2005). Conversely, other studies suggest that widths of streams through grassland are generally greater than those through forest (Charlton *et al.*, 1978; Hey and Thorne, 1986; Gregory and Gurnell, 1988; Rosgen, 1996). It should be noted that previous studies have categorized riparian vegetation in a multitude of ways, so it can be difficult to compare findings or make generalized conclusions. These apparently contrary findings may also be partially explained by a scale-dependent effect of riparian vegetation, such that in catchments greater than 10–100 km^2 widths are narrower when thick woody vegetation is present and in smaller catchments the opposite effect is observed (Anderson *et al.*, 2004). The driving mechanisms for these width adjustments are not well described or understood at either scale. If the channel processes associated with reforesting riparian zones were better understood, these conflicting findings might be resolved. An understanding of channel processes is also essential to properly guide stream-restoration activities (Hession, 2001).

The driving mechanisms that create these differences in channel size likely operate on a timescale greater than the length of a typical research study; therefore, field-based research opportunities are limited. Long-term channel change in response to riparian vegetation change has been documented in a couple of cases (Parkyn *et al.*, 2003; McBride *et al.*, 2005). The study in New Zealand evaluated channel response in small streams restored with forest buffers planted 2–24 years prior to the study (Parkyn *et al.*, 2003). Researchers did not find a significant difference in channel width between reforested and control reaches, and they suggest the plantings were too young to initiate widening (Parkyn *et al.*, 2003). A study comparing historic data from Zimmerman *et al.* (1967) and data collected nearly 40 years later in 2004 in the same stream reaches investigated differences in channel width over time (McBride *et al.*, 2005). The Zimmerman *et al.* (1967) study was one of the earliest on this subject and found that channel bed widths were larger in reaches with forested riparian vegetation than in reaches with 'sod' or grassy riparian vegetation for several small tributaries in the Sleepers River catchment. In the 1960s, this area had a diverse patchwork of forested and non-forested riparian vegetation, but since then approximately 1 km of these tributaries has passively reforested. These reforested stream reaches were significantly wider in 2004 than as measured in the 1960s (McBride *et al.*, 2005).

Several theories on the mechanisms driving channel widening have been postulated in the literature. The process of channel widening that presumably occurs following the reforestation of a riparian zone has been attributed to two main effects: (1) the suppression of grassy and understory vegetation on the banks and within channels with a closed canopy (Murgatroyd and Ternan, 1983; Davies-Colley, 1997) and (2) local scouring from large woody debris (LWD; Zimmerman *et al.*, 1967; Murgatroyd and Ternan, 1983; Trimble, 1997, 2004). Although Allmendinger *et al.* (2005) discussed differences in channel equilibrium widths of forested and non-forested streams related to different ratios between rates of cutbank erosion and deposition on active floodplains, the process of channel widening that presumably accompanies reforestation is not explained. Another possible mechanism for channel widening not yet explored is the hydraulic effect of forested vegetation during overbank flows. When flows overtop channel banks in reaches with forested floodplains, flows must circumvent tree trunks, resulting in more roughness than found on a non-forested floodplain. The hydraulic characteristics of overbank flows with forested versus non-forested floodplains are likely different, and the impact to channel morphology may be significant. Given the difficulties of monitoring and collecting data during infrequent overbank flow events on small streams with flashy flow regimes, a physical model provides an experimental surrogate for investigating the possible driving hydraulic conditions.

Flume studies offer the advantage of a controlled experimental environment where the hydraulic forces and channel response can be isolated, thereby avoiding some of the complications involved in field-based research (Thompson and Wohl, 1998). Several flume studies have investigated the hydraulic and geomorphic effects of vegetation, including studies of drag coefficients with submerged vegetation (Garcia *et al.*, 2004), changes in channel planform and dimensions (Gran and Paola, 2001; Bennett and Alonso, 2003) and hydrodynamic behavior and flow resistance (Pasche and Rouve, 1985; Naot *et al.*, 1996; Darby, 1999; Nezu and Onitsuka, 2001). To our knowledge, no physical model study has explored the hydraulic characteristics of overbank flows as a driving mechanism for channel widening in response to riparian reforestation using a scaled-model approach.

One key hydraulic behavior that may be driving channel widening is a shear-layer effect. A shear layer can establish itself at the interface between a main channel and a floodplain due to the velocity differential between the floodplain flow and the main channel flow (Shiono and Knight, 1991; Wormleaton, 1996). This type of shear layer is composed of periodic, whirlpool-like flow elements called vortices or coherent structures (Tritton, 1988; Smith, 1996). These zones of high shear have been identified in pools (Thompson, 2007) and at stream confluences (Biron *et al.*, 1993; McClelland *et al.*, 1996) and have been shown to significantly influence channel morphology. Studies of shear zones above submerged vegetation have shown intermittent organized vortices and maximum values of turbulence intensity

DOI: 10.1002/esp

and Reynolds shear stress near the top of the vegetation canopy (Ikeda and Kanazawa, 1996; Garcia *et al.*, 2004). The introduction of vegetation results in additional drag forces, turbulent energy and anisotropy of turbulence (Naot *et al.*, 1996). Consequently, many researchers have numerically described the channel–floodplain interface as an imaginary vertical wall to facilitate modeling techniques (Pasche and Rouve, 1985; Naot *et al.*, 1996). Visualization techniques show that intensive vortex shedding occurs at the channel–floodplain interface due to an intensive momentum exchange between two distinct regions of varying velocity (Pasche and Rouve, 1985).

We hypothesize that, during overbank flows, turbulence generated from riparian trees locally broadens stream reaches from a narrow, non-forested equilibrium size to a wider forested size. Flow separation around tree trunks along forested stream reaches will generate localized turbulence and scour that may increase channel width through bank erosion. Because trees are stable features that can fix the location of vortex shedding for years, turbulent scour along the bank may gradually increase channel width. In contrast, non-forested stream reaches typically contain fewer persistent obstructions that could generate turbulent scour. Our objective was to conduct a controlled flume experiment using a scaled model of a non-forested reach of an unnamed tributary to Sleepers River in northeastern Vermont. This tributary, stream W12, is significant because it was the site of an early investigation by Zimmerman *et al.* (1967) and has subsequently experienced reforestation of some riparian areas (McBride *et al.*, 2005). Overbank flows were simulated to investigate near-bank turbulence and flow dynamics that might be responsible for channel widening in response to a change in riparian vegetation.

Methods

Experimental specifications and procedure

Experiments were performed in a recirculating flume 1·0 m wide, 0·3 m deep and 6·0 m long at the University of Vermont's Hydraulics Laboratory. Discharge was measured using a calibrated Venturi meter installed in the flume's piping system. An adjustable tailgate at the downstream end of the flume controlled the water depth. Instruments were mounted from above on an aluminum plate carriage that traveled the length of the flume on stainless steel rails.

The base channel geometry for the experiments originated from a highly simplified, 1:5 scale model of W12 in the Sleepers River catchment (Figure 1). Channel width (at the crest of the bank), bank slope and channel cross-sectional area were all based on mean values derived from four cross-sectional field surveys of a *non-forested* reach of W12. The flume's gradient for all experimental runs was fixed at 0·03, the mean slope of W12, while other channel dimensions varied because of the different bank angles used in the experiment (Table I).

Figure 1. Non-forested reach of stream W12 (prototype). April 21, 2004. This figure is available in colour online at www.interscience.wiley.com/journal/espl

Table I. Experimental flume runs and channel dimensions

Run	Riparian vegetation	Bank angle	Discharge (L/s)	Bed width (cm)	Water depth (cm)	Channel width (cm)	Channel area (cm^2)
1	Forested	Angled	30	22·0	19·0	33·0	220·0
2	Forested	Angled	33	22·0	19·0	33·0	220·0
3	Forested	Angled	36	22·0	20·2	33·0	220·0
4	Forested	Vertical	30	33·0	18·5	33·0	264·0
5	Forested	Vertical	33	33·0	19·5	33·0	264·0
6	Forested	Vertical	36	33·0	19·5	33·0	264·0
7	Forested	Undercut	30	45·0	18·5	34·0	316·0
8	Forested	Undercut	33	45·0	19·0	34·0	316·0
9	Forested	Undercut	36	45·0	19·5	34·0	316·0
10	Non-forested	Angled	30	22·0	19·0	33·0	220·0
11	Non-forested	Angled	33	22·0	19·0	33·0	220·0
12	Non-forested	Angled	36	22·0	20·5	33·0	220·0
13	Non-forested	Vertical	30	33·0	18·5	33·0	264·0
14	Non-forested	Vertical	33	33·0	18·5	33·0	264·0
15	Non-forested	Vertical	36	33·0	20·5	33·0	264·0
16	Non-forested	Undercut	30	45·0	18·5	34·0	316·0
17	Non-forested	Undercut	33	45·0	19·0	34·0	316·0
18	Non-forested	Undercut	36	45·0	19·5	34·0	316·0

Six experimental stream morphologies were created in a test region of the flume measuring 367 cm long by 94 cm wide. Each experimental morphology was designed to represent half of a straight, uniform channel with an adjacent, flat floodplain (Figure 2). The width of the floodplain, 61 cm, was approximately double the channel width in the flume. One of the flume's vertical walls comprised the channel centerline. Although we would have preferred to model the entire channel with both sides of the floodplain, we were limited by the size of our flume and the minimum channel dimensions needed to collect data with our instrumentation. Two types of riparian vegetation were simulated on the floodplain surface: non-forested, with synthetic grass carpeting; and forested, where rigid, randomly distributed, wooden dowels were added (Figure 3). Because both the forested and non-forested experimental morphologies were the same size, we assumed the forested experimental morphologies were essentially under-fit, which permitted us to investigate hydraulic conditions during the crucial widening period. Three bank angles were simulated: angled (36°), vertical (90°) and undercut (144°).

The experimental channels and floodplains were constructed out of rigid, high-density polyethylene plastic sheets to create fixed boundaries. Channel bottom sections were roughened by attaching a single layer of 6 mm sorted pea gravel with construction adhesive. The pea gravel was sorted to achieve the 1:5 ratio with the median sediment size (30 mm) of W12. Channel banks were similarly glued with a layer of fine sand (approximately 0·125 to 0·25 mm), roughly one-fifth the size of the course sand found in the prototype's stream banks. The floodplain surface was affixed with 1 cm thick synthetic grass carpet for all experimental runs. Dowels had been successfully used in several flume experiments to simulate trees or other vegetation (Pasche and Rouve, 1985; Tsujimoto, 1996; Nezu and Onitsuka, 2001; Garcia *et al.*, 2004). Therefore, for runs with forested riparian vegetation, rigid wooden dowels 2·5 cm in diameter were attached from the underside of the floodplain surface in a random configuration. Dowel diameter and spacing, both along the bank and throughout the floodplain, were scaled from measurements of a 10 m^2 plot of riparian forest at W12. The spacing of dowels was denser along the bank to mimic our field observations of a clustering of water-tolerant tree species along the bank crest.

A total of 18 flume runs were conducted with all combinations of riparian vegetation, bank angle and discharge (Table I). Experiments were run at three different discharges: 30, 33 and 36 L/s. These discharges corresponded to overbank flows in W12 with discharges of 3·35, 3·69 and 4·02 m^3/s, based on dynamic, Froude similitude (Chanson, 1999). Limited hydrologic data are available for W12; however, a maximum peak discharge of 0·59 m^3/s was recorded between 1963 and 1966 (Zimmerman *et al.*, 1967). We measured a spring-melt peak discharge of 0·21 m^3/s at W12 on 6 April 2005, but this flow event was contained within the channel. To roughly estimate the return interval of the modeled discharges, we used a United States Geologic Survey (USGS) area-based regression method for ungaged streams (Johnson and Laraway, 1971). Several area-based methods are applicable for Vermont (VTAOT, 1998); however, the USGS method provided an estimate of the 2-year peak discharge (0·79 m^3/s) that most closely matched

DOI: 10.1002/esp

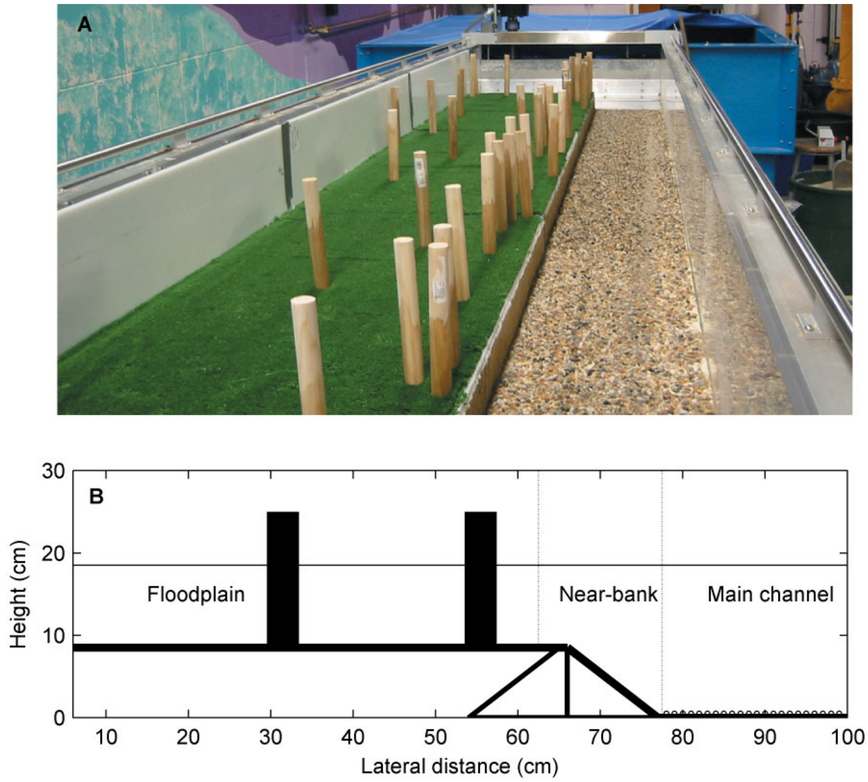

Figure 2. Experimental flume set-up shown with an oblique photograph of a forested run with vertical banks (a) and in cross-section with three bank angles shown overlapping (b). Flow direction is into the page. This figure is available in colour online at www.interscience.wiley.com/journal/espl

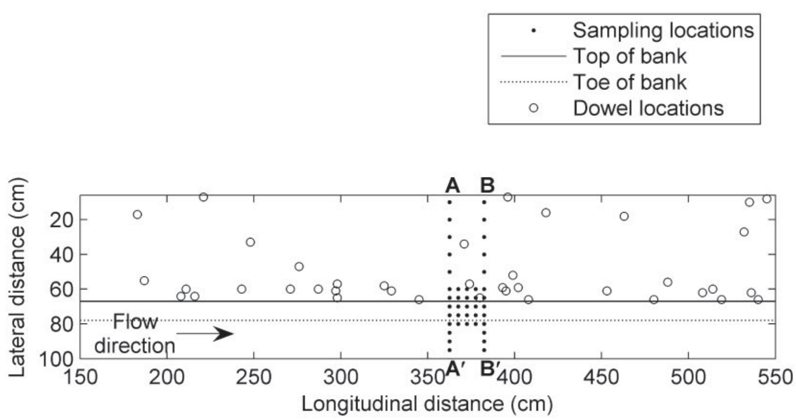

Figure 3. Plan-view of experimental flume set-up.

the measured peak flow in the 1960s. Using this method, we found our simulated discharges approximately equaled the 50-year peak discharge (3·48 m^3/s). Although we would have preferred to simulate smaller, more frequent floods, our instrumentation required a minimum water depth to enable the collection of velocity measurements. We assume that the hydraulic characteristics and flow patterns will be similar for most overbank flows at different stages, but that the magnitude of velocities and velocity-derived parameters will vary based on discharge.

DOI: 10.1002/esp

The tailgate of the flume was maintained at a constant height for all 18 experimental runs to maintain subcritical flow throughout the test region of the flume and to ensure a minimum water depth of at least 8 cm on the floodplain surface. Froude similitude was achieved and confirmed by a comparison of the Froude number calculated from the 6 April discharge in W12 (0·37) and the Froude number attained in the main channel portion of the flume (0·38–0·39).

Three-dimensional velocities were measured with a Nortek Vectrino acoustic Doppler velocimeter (ADV; Annapolis, MD). The ADV is a downward-oriented probe that employs the Doppler effect, sending sound pulses from its central transducer that are reflected by suspended particles and collected by four receivers. The sampling volume was 0·2 cm^3, located 5 cm below the probe. Levels were attached to the ADV to ensure that the equipment was properly and consistently mounted. Seeding material composed of 8–13 μm borosilicate glass beads was used during all experimental runs to ensure quality measurements. The ADV sampled at a rate of 25 Hz for at least 90 s for each measurement. Post-processing of the three-dimensional velocity components showed that stationarity was attained well within a 90 s recording time.

Three-dimensional velocities were measured at 41 locations within the main channel and floodplain at near-bed (approximately 1 cm from the bottom surface) and 0·6-depth elevations. Measurement locations were configured in two cross-sections (A–A′ and B–B′) and in a 20 cm by 20 cm region between the two cross-sections (Figure 3). Along each cross-section, measurement locations were spaced every 10 cm in the floodplain region and every 5 cm within the near-bank and main channel regions. In the region between cross-sections, velocities were collected on a 5 cm grid. At all 41 locations, velocities were sampled at near-bed depth. Furthermore, the deeper water in the main channel and near-bank regions permitted additional velocity measurements conducted at the 0·6-depth. In the runs with the forested floodplain, it was not possible to sample at two locations because they were obscured by dowels.

Analytical methods

Data filtering. Post-processing methods were used to ensure quality data and the best representation of true velocity conditions. Erroneous data due to communication errors, low signal correlation, low signal-to-noise ratios (SNR) or effects of aliasing can bias mean velocity values and turbulence statistics (Lane *et al.*, 1998). Instantaneous velocities were discarded if the signal correlation dropped below 0·7 or if SNR values dropped below 15 dB (Lane *et al.*, 1998; Wahl, 2000). Although removing erroneous velocities is beneficial, the removal of too many data can be counterproductive because the true variance may be reduced. Consequently, we eliminated any velocity files if more than 15 per cent of the instantaneous velocity values were discarded (Lane *et al.*, 1998). A total of 1100 velocity files were recorded during the 18 flume runs, and of these only four files were discarded. The four discarded velocity files were collected during forested flume runs at a location adjacent to one of the wooden dowels (cross-section B–B′ at 65 cm). Low correlation values in these four files were likely caused by interference from the dowel. Of the remaining files, the mean percentage of retained points was 99·1 per cent. The files were filtered with a Gaussian low-pass filter to a frequency of 12·5 Hz to eliminate Doppler noise (Lane *et al.*, 1998). Post-processing of velocity data was completed using ExploreV software from NortekUSA (Annapolis, MD).

Key parameters. Following data post-processing, several parameters were calculated from the velocity measurements including mean velocities in the streamwise (U), lateral (V) and vertical (W) directions, turbulent kinetic energy (TKE), Reynolds shear stresses (R_l and R_v) and boundary shear stress (τ_p). Because the short-term variation of velocities around their time-averaged values is an essential aspect of turbulent motion, the intensity of turbulence can be quantified as

$$\mathrm{TKE} = 0{\cdot}5\rho(\langle u'^2\rangle + \langle v'^2\rangle + \langle w'^2\rangle) \tag{1}$$

where ρ is the density of water and $\langle u'^2\rangle$, $\langle v'^2\rangle$ and $\langle w'^2\rangle$ are the mean square differences between the instantaneous velocities and the time-averaged velocities in the streamwise, lateral and vertical directions, respectively (Bradshaw *et al.*, 1967; Clifford and French, 1993). We determined Reynolds fluctuating shear stress in the lateral direction:

$$R_l = -\rho(\langle u'v'\rangle) \tag{2}$$

and in the vertical direction

$$R_v = -\rho(\langle u'w'\rangle) \tag{3}$$

DOI: 10.1002/esp

where <*u′v′*> is the mean of the product of the fluctuations of streamwise and lateral velocities and <*u′w′*> is the mean of the product of the fluctuations of streamwise and vertical velocities (Clifford and French, 1993). Reynolds shear stresses were calculated to investigate the character of the turbulence in the near-bank region, and a quadrant analysis of those stresses was used to dissect the velocity signal based on the relative signs of u', v' and w' (Lu and Willmarth, 1973). To explore potential impacts of turbulence on the channel morphology of the prototype stream, values of boundary shear stress were calculated such that

$$\tau_{\mathrm{p}} = \frac{\rho_{\mathrm{p}}}{\rho_{\mathrm{m}}} L_{\mathrm{r}} \left[\frac{c\mathrm{TKE}_{\mathrm{m}}}{\left(1 - \frac{1}{s^2}\right)^{1/2}} \right] \qquad (4)$$

where subscripts 'p' and 'm' correspond to prototype (stream) and model values, respectively. L_r is the length ratio of the prototype channel to the model, c is a proportionality constant assumed to be 0·21 (Daniels and Rhoads, 2004) and s is the side slope (1:s, vertical:horizontal). The side slope, s, in the denominator adjusts for the increased length of the bank surface with angled banks (runs 1–3 and 10–12). The simple linear relationship between boundary shear stress (τ_p) and TKE was successfully demonstrated in tidal currents, stream channels and flume applications (Kim *et al.*, 2000; Biron *et al.*, 2004; Daniels and Rhoads, 2004). Water temperatures in the flume ranged from 23 to 26 °C and the corresponding ρ values (0·9975–0·9967 g/cm^3) were used in the calculation of TKE, Reynolds shear stress and boundary shear stress. Water temperature in W12 was assumed to be 5 °C with ρ equal to 1·0000 g/cm^3.

Statistical methods. Parametric statistical techniques were used to test for differences in mean values of the measured parameters. Separate analyses were performed in each of three distinct regions of the flume: floodplain (6–62·5 cm); near bank (62·5–77·5 cm) and main channel (77·5–100 cm; Figure 2). All parameters were found to be approximately normally distributed by the inspection of normal quantile plots and the Shapiro–Wilk test (JMP, 2002). A randomized complete block approach was used to test for differences in velocity components, TKE and Reynolds shear stress. Each measurement location (Figure 3) was treated as a block with riparian vegetation, bank angle and discharge level as fixed factors. Results were examined for interaction effects, where the effect of one factor might not be independent of the particular level of another factor (Zar, 1999). Blocks with missing data were excluded from the analysis. This approach was preferred over a simpler factorial analysis of variance because replicates were not independent due to strong spatial correlation between adjacent measurement locations. Statistical testing was completed using JMP software v.5.0.1.2 (SAS Institute, Cary, NC).

Results

Values of velocities and TKE throughout the sampled cross-section of the flume varied depending on location, riparian vegetation type, discharge and bank angle. Plan-view plots of the sampled area display near-bed velocities with vectors and near-bed TKE in shaded contours for runs 2 and 11 (Figure 4). Trends in these figures are generally representative of results from all runs. In the forested scenario, a narrow band of high TKE values was apparent at approximately 70 cm in the cross-section, occurring at the interface between the floodplain and the main channel, with values more than double those observed in the corresponding non-forested run. In the non-forested scenario, the highest TKE values occur on the floodplain with additional bands of elevated TKE at 70 and 90 cm. Both figures demonstrated the dominant streamwise velocities, and substantially higher velocities in the main channel versus the floodplain.

Lateral and vertical velocity vectors are shown in cross-section plots (Figure 5(a) and (b)), and are generally similar for both forested and non-forested runs. Velocity vectors in the non-forested run display small lateral currents smoothly flowing from the floodplain to the main channel; however, velocity vectors in the forested run are more complicated, especially in the near-bank region. Although it was not possible to measure velocities near the water surface due to limitations of the downward-facing probe, secondary circulation is presumed, such that surface velocities would be directed back to the floodplain in both forested and non-forested runs. Compound channels commonly exhibit multiple regions of secondary circulation (Wormleaton, 1996; Nezu, 2005). Deviations from these general trends and detailed findings including interactions between factors for subsequent flume runs are described below by region (floodplain, near-bank and main channel). Due to the experimental design with three fixed factors (riparian vegetation, bank angle and discharge), results were multifaceted and, commonly, the response of the system to one factor was dependent on the levels of the other factors.

DOI: 10.1002/esp

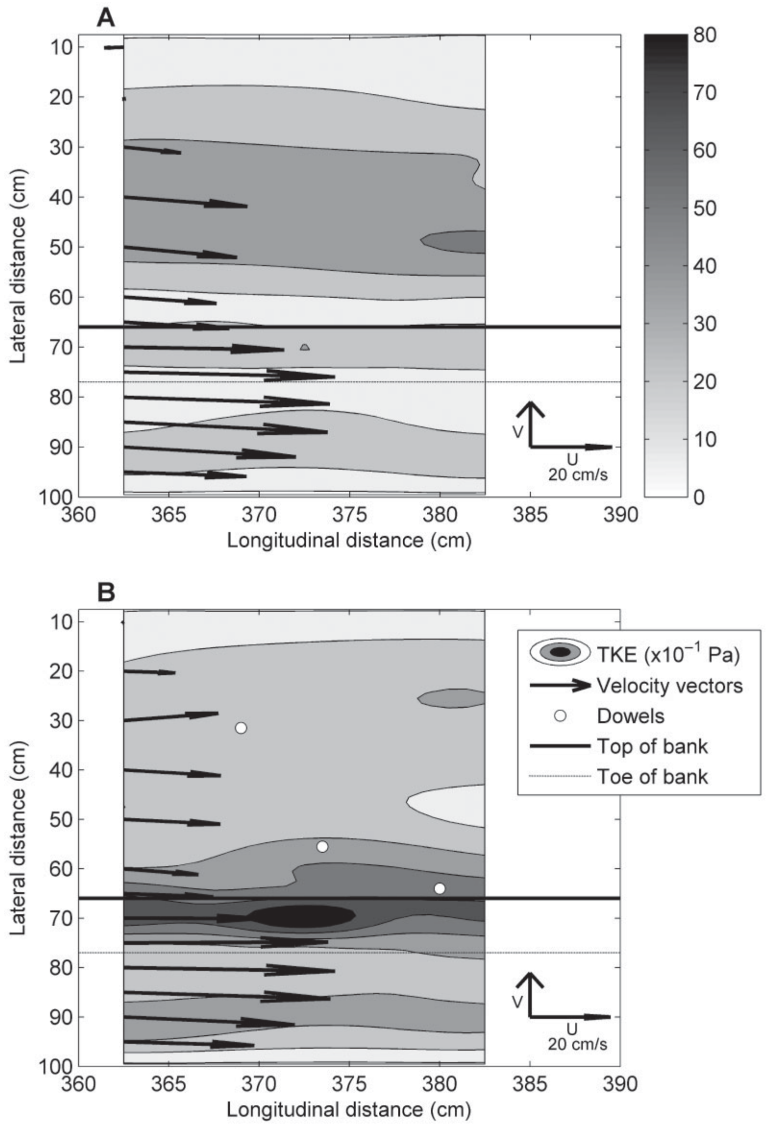

Figure 4. Plan-view contour maps of TKE values ($\times 10^{-1}$ Pa) in non-forested run 11 (a) and forested run 2 (b) with angled banks and 33 L/s discharge. Velocity vectors are shown for cross-section A-A.

Floodplain region

Velocities and TKE in the floodplain region exhibited minor differences between forested and non-forested runs (Table II). In both forested and non-forested runs, streamwise velocities increased significantly with increasing discharge, and lateral velocities were directed toward the main channel. Non-forested runs had significantly greater lateral velocities along the bed than forested runs. In forested runs TKE values increased directly with discharge, whereas in non-forested runs TKE values exhibited less change (Figure 6(a)). Examination of this interaction effect showed that under the lowest-discharge regime non-forested runs (10, 13 and 16) had greater TKE values than the forested runs (1, 4 and 7); however, under the higher discharge regimes forested runs exhibited greater TKE. Differences in vertical velocities between forested and non-forested runs were negligible, even though there was a significant interaction between riparian vegetation and bank angle.

DOI: 10.1002/esp

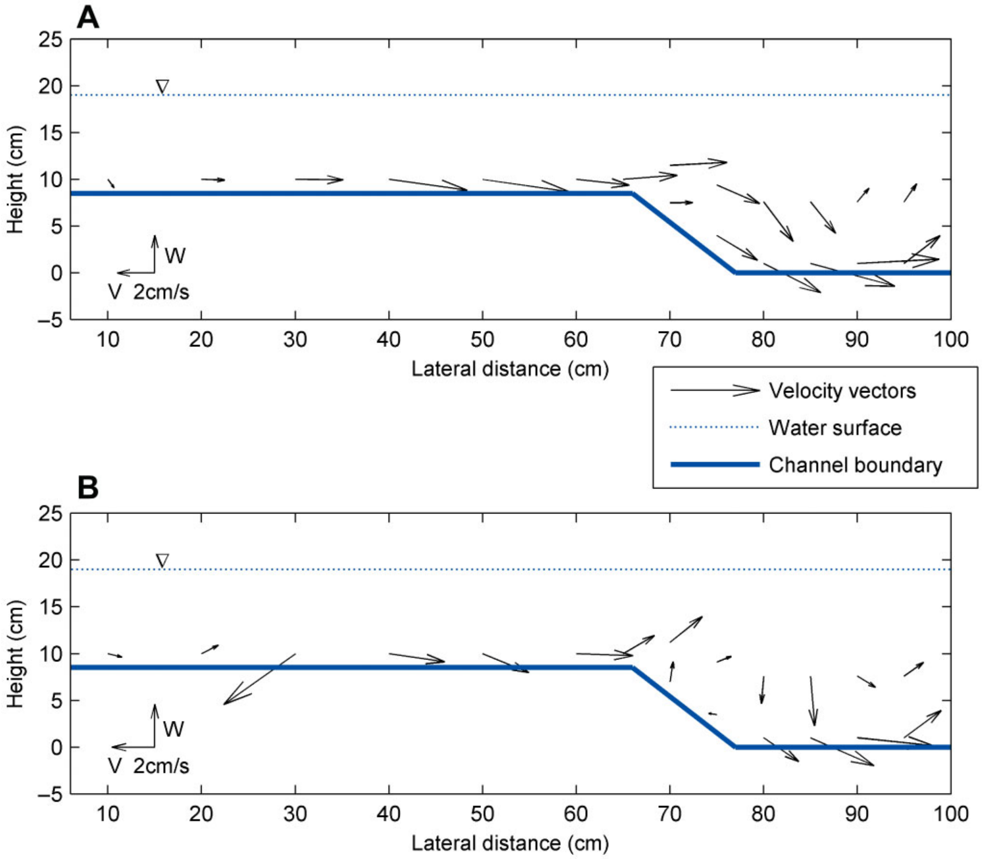

Figure 5. Cross-section views of lateral (V) and vertical velocities (W) in non-forested run 11 (a) and forested run 2 (b). Both runs had angled banks and 33 L/s discharge. This figure is available in colour online at www.interscience.wiley.com/journal/espl

Table II. Results of the randomized complete block analysis of the floodplain region (14 blocks). Bold values are significant at the 95% confidence level

Factors	Levels	*U* (cm/s) Mean	*U* (cm/s) *p*-value	*V* (cm/s) Mean	*V* (cm/s) *p*-value	*W* (cm/s) Mean	*W* (cm/s) *p*-value	TKE (× 10⁻¹ Pa) Mean	TKE (× 10⁻¹ Pa) *p*-value
Riparian	forest	17·60	0·4413	**−1·12**	**<0·0001**	−0·18	*	27·70	*
vegetation	non-forest	17·04		**−2·28**		−0·21		29·35	
Bank angle	angled	16·40	0·0606	−1·71	0·1553	−0·26	*	27·01	0·3209
	vertical	18·46		−1·52		−0·16		28·82	
	undercut	17·09		−1·87		−0·16		29·74	
Discharge	30	**14·99**	**<0·0001**	−1·78	0·6759	−0·21	0·8236	26·95	*
	33	**17·49**		−1·71		−0·20		28·41	
	36	**19·47**		−1·62		−0·17		30·21	
Interactions									
Rip. veg. × bank			0·2316		0·8732		**0·0252**		0·5374
Rip. veg. × discharge			0·9468		0·5236		0·7423		**0·0032**
Bank × discharge			0·9999		0·4430		0·9771		0·5180
Rip. veg. × bank × discharge			0·9998		0·7884		0·9340		0·9910

* *p*-values are excluded when interaction effects are significant and interpretations of mean values must consider interaction effects.

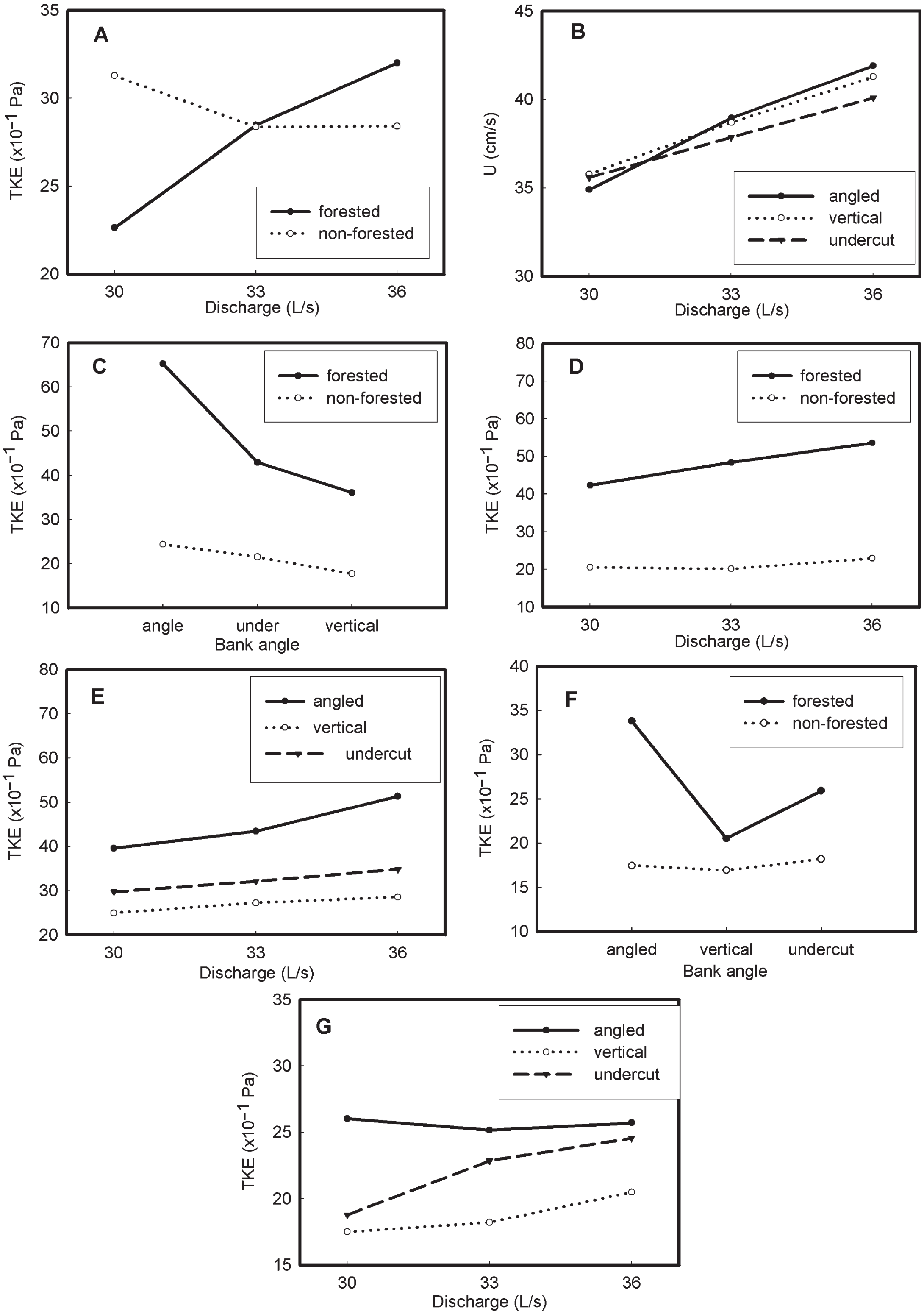

Figure 6. Plots of mean values of TKE and of streamwise velocity (U) to display trends with factors that interacted significantly in the floodplain region (a,b), the near-bank region (c-e), and the main channel region (f,g).

Table III. Results of the randomized complete block analysis of the near-bank region (23 blocks). Bold values are significant at the 95% confidence level

Factors	Levels	*U* (cm/s) Mean	*U* (cm/s) *p*-value	*V* (cm/s) Mean	*V* (cm/s) *p*-value	*W* (cm/s) Mean	*W* (cm/s) *p*-value	TKE ($\times 10^{-1}$ Pa) Mean	TKE ($\times 10^{-1}$ Pa) *p*-value
Riparian	forest	**36·87**	**<0·0001**	−0·25	*	**0·21**	**<0·0001**	48·12	*
vegetation	non-forest	**39·80**		−2·11		**−0·47**		21·99	
Bank angle	angled	38·58	*	−1·19	*	**0·12**	**<0·0001**	44·81	*
	vertical	38·58		−1·00		**0·02**		26·92	
	undercut	37·84		−1·35		**−0·53**		32·24	
Discharge	30	35·42	*	−1·49	*	**−0·01**	**<0·0001**	31·43	*
	33	38·49		−1·40		**−0·14**		34·29	
	36	41·09		−0·65		**−0·24**		38·25	
Interactions									
Rip. veg. × bank			0·0806		*		0·0645		**<0·0001**
Rip. veg. × discharge			0·2053		*		0·3280		**<0·0001**
Bank × discharge			**0·0286**		*		0·8276		**0·0016**
Rip. veg. × bank × discharge			0·3899		**<0·0001**		0·1672		0·1636

* *p*-values are excluded when interaction effects are significant and interpretations of mean values must consider interaction effects.

Near-bank region

Results in the near-bank region are more complex than either the floodplain or main channel regions; differences in velocities and TKE between forested and non-forested runs were substantial (Table III). Non-forested runs had significantly greater streamwise velocities than forested runs. Additionally, the velocity vectors in Figure 4 illustrated a gradual gradient in streamwise velocity in the non-forested run, while the streamwise velocity increased more rapidly between the 70 and 75 cm locations in the forested run. Non-forested runs had greater lateral velocities and stronger, downward-oriented vertical velocities than forested runs, which had positive vertical velocities (i.e., upward oriented). Although velocities were generally greater in the non-forested runs in the near-bank region, the magnitude of TKE in forested runs was consistently more than twice that of the non-forested runs, regardless of bank angle (Figure 6(c)) or discharge (Figure 6(d)). The distribution of TKE in the water column, as measured at 0·6 depths and at the bed, was different between forested and non-forested runs. In non-forested runs, TKE was almost always greater along the bed than at 0·6 depths (Figure 7(a)). In forested runs, TKE at 0·6 depths was nearly equivalent or greater than TKE along the bed (Figure 7(b)).

Both bank angle and discharge level affected many of the velocity components and TKE. Streamwise velocities increased with discharge for all bank types; however, angled banks had the greatest increase with discharge (Figure 6(b)). Lateral velocities had a significant three-factor interaction, indicating that riparian vegetation, bank angle and discharge were interrelated in their effect on this parameter, but they did not exhibit any notable trends. Vertical velocities were significantly influenced by each factor individually. Angled banks resulted in upward-oriented vertical velocities, undercut banks resulted in downward-oriented vertical velocities and vertical banks had negligible vertical velocities. Neither bank angle nor discharge level had a sizeable effect on TKE values in non-forested runs (Figure 6(c) and (d)); however, in forested runs, TKE values increased with increasing discharge, and TKE values were higher with an angled bank (Figure 6(c) and (d)). For all bank types TKE increased with increasing discharge and angled banks had higher TKE overall (Figure 6(e)).

The peak turbulence in forested runs occurs along the bank face at 70 cm (Figure 7(b)) and an analysis of Reynolds shear stresses at that location illustrated differences between forested and non-forested runs (Table IV). When two typical runs were compared, the forested run (run 2) had over three times greater mean lateral Reynolds shear stress and over two times greater mean vertical Reynolds shear stress than the corresponding non-forested run (run 11). Quadrant analysis showed that the forested run had the highest values of lateral Reynolds shear stress in quadrant 1, where $u' > 0$, $v' > 0$, and quadrant 3, where $u' < 0$, $v' < 0$. Moreover, 40 per cent of the time was spent in quadrant 1, which corresponds to greater than average streamwise velocities directed toward the bank face ($u' > 0$, $v' > 0$). The velocity signal in the non-forested run showed a similar pattern in time distribution, but the absolute values of lateral Reynolds shear stress were much smaller in each quadrant. Quadrant analysis of the vertical Reynolds shear stress

DOI: 10.1002/esp

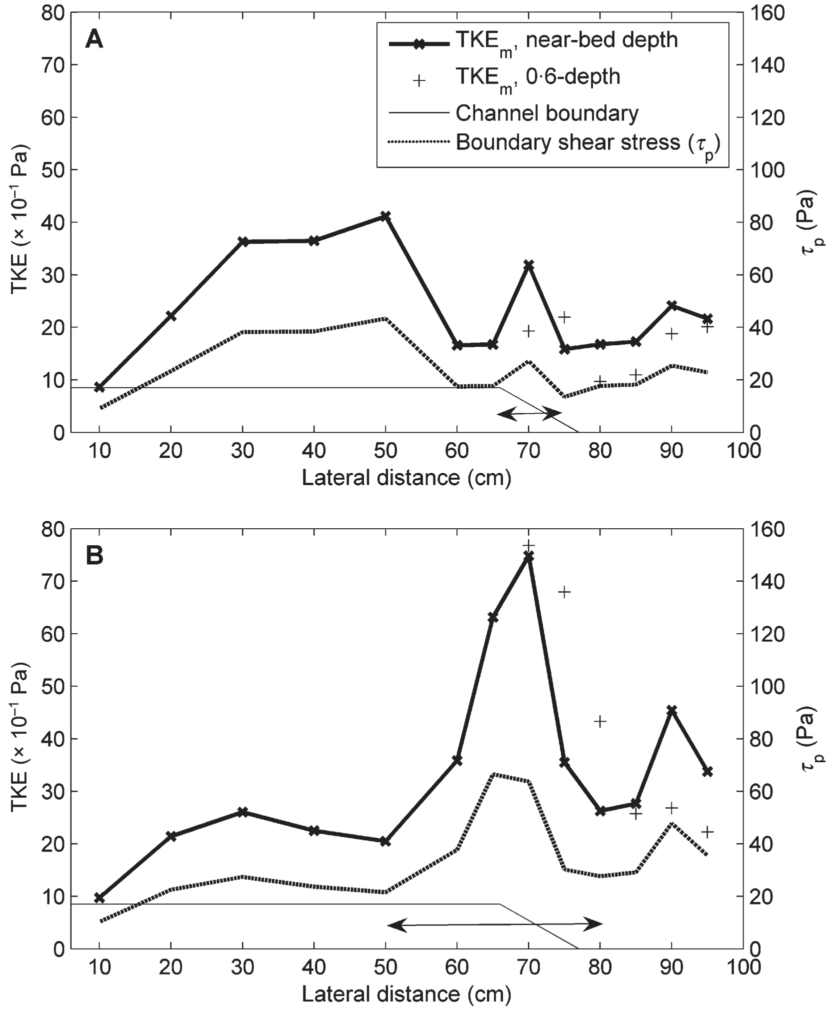

Figure 7. TKE values (of model) and boundary shear stresses (of prototype) at cross-section A-A' for non-forested run 11 (a) and forested run 2 (b). Shear layer widths are identified with arrows.

showed that the stress and the percentage of time were fairly evenly distributed in the four quadrants for both forested and non-forested runs.

Main channel region

Although the geometry and roughness of the main channel region were identical throughout the 18 flume runs, velocities and TKE were influenced by changes in riparian vegetation and bank angle in the other regions (Table V). In both forested and non-forested runs, streamwise velocities increased significantly with increasing discharge and vertical velocities were consistently negative. Streamwise velocities were also higher with angled banks as compared to vertical or undercut banks, likely due to the smaller capacity of the cross-section. Lateral velocities had a significant three-factor interaction, indicating that each combination of riparian vegetation type, bank angle and discharge yielded different results without any apparent trends. Forested runs had greater TKE values than non-forested runs for any given bank angle and discharge level; however, TKE results exhibited significant interaction effects between some factors. Bank angle did not have a sizeable effect on TKE values in non-forested runs, but in forested runs the angled bank promoted the greatest turbulence, followed by undercut banks and vertical banks (Figure 6(f)). Closer inspection of the bank angle and discharge interaction effect revealed stable TKE values with discharge for the angled bank; however, both undercut and vertical banks showed an increase in TKE with increasing discharge (Figure 6(g)).

Table IV. Distribution of Reynolds shear stresses and percentage of time (in parentheses) by quadrant for two runs from measurements at location 70 cm along cross-section A–A′

		Forested (run 2)	Non-forested (run 11)
Mean velocities			
	U	34·5	39·4
	V	−0·1	−1·2
	W	0·9	0·0
Lateral Reynolds shear stress	Quadrants		
	1 $u' > 0, v' > 0$	−51·3 (40%)	−17·5 (37%)
	2 $u' < 0, v' > 0$	17·6 (13%)	7·1 (15%)
	3 $u' < 0, v' < 0$	−72·6 (36%)	−26·6 (34%)
	4 $u' > 0, v' < 0$	14·8 (11%)	6·9 (14%)
	Total mean	−42·8	−13·3
Vertical Reynolds shear stress	Quadrants		
	1 $u' > 0, w' > 0$	−27·1 (31%)	−13·2 (33%)
	2 $u' < 0, w' > 0$	19·3 (20%)	8·0 (18%)
	3 $u' < 0, w' < 0$	−34·0 (29%)	−15·6 (31%)
	4 $u' > 0, w' < 0$	16·2 (20%)	6·7 (18%)
	Total mean	−10·9	−6·5

Table V. Results of the randomized complete block analysis of the main channel region (22 blocks). Bold values are significant at the 95% confidence level

		U (cm/s)		V (cm/s)		W (cm/s)		TKE ($\times 10^{-1}$ Pa)	
Factors	Levels	Mean	p-value	Mean	p-value	Mean	p-value	Mean	p-value
Riparian	forest	44·74	*	−0·61	*	−0·69	0·1487	26·75	*
vegetation	non-forest	44·25		−2·15		−0·62		17·54	
Bank angle	angled	48·31	*	−1·32	*	−0·72	0·1337	25·64	*
	vertical	42·95		−1·16		−0·64		18·73	
	undercut	42·21		−1·66		−0·60		22·06	
Discharge	30	**42·64**	**<0·0001**	−1·57	*	−0·65	0·6347	20·77	*
	33	**44·84**		−1·64		−0·70		22·07	
	36	**46·00**		−0·94		−0·62		23·58	
Interactions									
Rip. veg. × bank			**<0·0001**		*		0·5446		**<0·0001**
Rip. veg. × discharge			0·2188		*		0·9961		0·4398
Bank × discharge			0·2522		*		0·8869		**0·0020**
Rip. veg. × bank × discharge			0·1545		**<0·0001**		0·9947		0·0873

* p-values are excluded when interaction effects are significant and interpretations of mean values must consider interaction effects.

Shear layer width

Estimations of the shear layer width were slightly limited by the 5 cm measurement spacing in the near-bank region. However, approximations of shear layer widths, as measured from the local minima on either side of the maximum TKE value in the near-bank region, were much greater in forested than in non-forested runs with angled banks (Table VI, Figure 7). The mean shear layer width approximation in forested, angled-bank runs was 36·7 cm, double the mean value for similar non-forested runs (18·3 cm). In non-forested runs with vertical or undercut banks, there were no local maxima at the interface of the floodplain and the main channel.

Table VI. Estimated bounds and width of the shear layer for the six experimental runs with angled banks

Riparian vegetation	Discharge (L/s)	Cross-section	Local minimum – floodplain (cm)	Local minimum – main channel (cm)	Shear layer width (cm)
Non-forested	30	A–A′	65	85	20
		B–B′	65	85	20
	33	A–A′	60	75	15
		B–B′	65	85	20
	36	A–A′	60	75	15
		B–B′	60	80	20
Forested	30	A–A′	50	85	35
		B–B′	50	80	30
	33	A–A′	50	80	30
		B–B′	50	85	35
	36	A–A′	40	85	45
		B–B′	40	85	45

Local maxima of TKE occur at 70 cm in each run.

Table VII. Mean velocities and boundary shear stresses in near-bank region of prototype channel

Run	Run description	U (m/s)	V (m/s)	W (m/s)	τ_p (Pa)
1	Forested, angled, 30 L/s	0·69	−0·03	0·01	47·76
2	Forested, angled, 33 L/s	0·75	−0·03	0·02	51·42
3	Forested, angled, 36 L/s	0·83	−0·01	0·01	62·81
4	Forested, vertical, 30 L/s	0·72	−0·02	0·02	30·51
5	Forested, vertical, 33 L/s	0·78	−0·01	0·02	35·14
6	Forested, vertical, 36 L/s	0·82	−0·01	0·02	34·88
7	Forested, undercut, 30 L/s	0·74	−0·03	0·01	35·69
8	Forested, undercut, 33 L/s	0·81	−0·04	0·01	46·37
9	Forested, undercut, 36 L/s	0·85	0·04	0·00	49·75
10	Non-forested, angled, 30 L/s	0·73	−0·06	0·00	19·44
11	Non-forested, angled, 33 L/s	0·83	−0·06	−0·01	20·73
12	Non-forested, angled, 36 L/s	0·90	−0·05	0·00	25·90
13	Non-forested, vertical, 30 L/s	0·80	−0·06	0·00	16·47
14	Non-forested, vertical, 33 L/s	0·86	−0·06	0·00	15·91
15	Non-forested, vertical, 36 L/s	0·94	−0·03	−0·01	16·10
16	Non-forested, undercut, 30 L/s	0·81	−0·10	−0·01	21·53
17	Non-forested, undercut, 33 L/s	0·86	−0·08	−0·02	19·20
18	Non-forested, undercut, 36 L/s	0·94	−0·09	−0·02	20·45

Boundary shear stress

Estimates of boundary shear stress in the near-bank region range from 15·91 to 62·81 Pa (Table VII). We have expressed boundary shear stress in terms of the expected values in the prototype channel (W12), to facilitate comparisons with field-based measurements of typical critical boundary shear stresses of various bank materials. Boundary shear stress was correlated with TKE results because of the direct relationship between these two parameters (Equation (4), Figure 7). Boundary shear stress was approximately twice as high in forested runs as in corresponding non-forested runs, and in forested runs boundary shear stress was at a maximum in the near-bank region.

Discussion

Our results strongly suggest that near-bank turbulence during overbank flow events could be enhanced in stream reaches transitioning from non-forested to forested riparian vegetation. Forested runs and non-forested runs were

DOI: 10.1002/esp

differentiated by the magnitude and patterns of TKE. In forested runs, a narrow band of high TKE values formed longitudinally in the flow above the bank surface (Figure 4(b)), which corresponded well to previous findings on the distribution of TKE throughout a cross-section with a vegetated floodplain (Pasche and Rouve, 1985; Naot *et al.*, 1996). Nezu and Onitsuka (2001) found that turbulence intensity of the streamwise velocity component and lateral Reynolds shear stresses were at a maximum at the interface of a vegetated and a non-vegetated zone in a flat-bottom channel. The orientation of the high-TKE band running parallel to the bank indicated that a highly turbulent shear layer established at the interface of the floodplain and main channel. In non-forested runs, a similar peak of TKE occurred along the bank surface, but it was much smaller than the TKE values measured in forested runs. High TKE values were found on the floodplain surface in non-forested runs likely due to bed shear (Table II; Figure 4(a)). Similarly, patterns in TKE at 0·6 depth versus near-bed depth suggested that TKE was driven primarily by bed roughness in the non-forested runs, whereas in forested runs TKE was elevated throughout the water column, probably due to larger vortices forming along the shear layer (Figure 7). Horizontal vortices at the interface of a vegetated and a non-vegetated zone have been observed and mapped using high-resolution velocity data in flume experiments (Nezu and Onitsuka, 2001). Additionally, in forested runs, flow separation caused by the dowels likely redirects high-momentum fluid from the upper portion of the water column down toward the bed.

High turbulence in the near-bank region should be a direct function of the velocity difference (Tinkler, 1997) and the magnitude of the resulting shear (Tennekes and Lumley, 1994) between the floodplain flow and the main channel flow. From similar research results, we expected reduced velocities in the forested floodplain and, consequently, a larger velocity differential as compared with the non-forested runs (Tsujimoto, 1996; Nezu and Onitsuka, 2001). Contrarily, streamwise velocities were not significantly reduced in the forested runs in the floodplain region when measured at near-bed depths (Table II). The added resistance of the dowels in forested runs may have reduced floodplain velocities in the upper portion of the water column, but we were unable to collect a velocity profile with our downward-facing probe. There was a greater velocity differential for forested runs than non-forested runs between the near-bank and main channel regions; for forested runs the difference in mean streamwise velocities was nearly 8 cm/s, while for non-forested runs the difference was approximately 4 cm/s (Tables III and V).

Forested and non-forested runs exhibited differences in the spatial extent of the shear layer. Estimated shear layer width was substantially larger in forested runs than in non-forested runs (Table VI), extending from mid-floodplain into the main channel (Figure 7(b)). Our observations of a pronounced peak of TKE values at approximately 70 cm laterally (Figures 4(b) and 7(b)), coupled with a wider shear layer in the forested runs, is likely a result of the energy cascade, where large vortices decay into progressively smaller vortices (Tritton, 1988). One of the interaction effects also indicates the effect of greater momentum transfer; in forested runs, bank angle strongly influenced TKE values in the main channel region, but had no such effect in non-forested runs (Figure 6(f)). This correlation of TKE values in the near-bank and main channel regions in forested runs is likely due to the mixing caused by the energy cascade.

Effects of discharge

The key result of the variable discharge runs was that, although the magnitudes of turbulence and velocities changed with discharge level, the pattern and distribution of these parameters did not change. Therefore, we might expect the same hydraulic effects, given more frequent, smaller overbank flow events but smaller magnitudes overall. In most cases, an increase in discharge corresponded to an increase in streamwise velocities and TKE. A notable exception was observed with TKE in the floodplain region. In non-forested runs, TKE decreased slightly with increasing discharge, suggesting that the turbulence caused by the synthetic grass layer was reduced with increasing water level. Conversely, in forested runs, where dowels were persistent obstructions, TKE increased with increasing discharge, suggesting that vortex shedding was apparently augmented with increased discharge.

Effects of bank angle

Three bank angles were included in the experimental design to simulate a progression of bank erosion that might coincide with channel widening (i.e. from angled to vertical to undercut). Although some researchers found that bank angle was not of great importance in experiments with a vegetated floodplain (Pasche and Rouve, 1985), bank angle was a significant factor in our results. With an angled bank, streamwise velocities and TKE were maximized within the channel (Figure 6(c) and (f)), likely due to the small cross-sectional area. TKE was greater for undercut than vertical banks (Figure 6(f)), because undercut banks likely promoted additional turbulence from complex flow patterns around the overhanging obstruction. Given that TKE in forested runs decreased significantly when the cross-sectional area was increased (with vertical and undercut banks) and given that our experimental channels were under-fit for a typical forested stream reach, we suspect that turbulence will become less exaggerated as a forested stream reach

DOI: 10.1002/esp

widens to its equilibrium size. A wider channel will decrease main channel flows due to its greater conveyance, which will, in turn, decrease the velocity differential and associated shear with floodplain flows.

Implications for channel widening

Exaggerated turbulence generated from a forested floodplain during overbank flows may be a key driving mechanism responsible for differences in channel width in stream reaches with different riparian vegetation. Because turbulence creates instantaneous forces much greater than time-averaged values, sediment transport can occur at flows where the time-averaged conditions are below the critical entrainment threshold for sediments (Nelson *et al.*, 1993; McLean *et al.*, 1994; Roy *et al.*, 1999). When increased turbulence is coupled with high downstream velocities, entrainment and transport of bank sediments are likely amplified (Thompson, 2004). Our experiment illustrated that when forested vegetation is added to the floodplain of a small, previously non-forested stream, turbulence is strongly amplified along a wide area between the floodplain and the main channel, including the entire bank face (Figure 7(b)). This adds another feasible mechanism to the two predominant ideas that channel widening in reforested reaches is a result of scour around LWD and bank weakness due to the suppression of grassy and understory vegetation (Zimmerman *et al.*, 1967; Murgatroyd and Ternan, 1983; Davies-Colley, 1997; Trimble, 1997, 2004).

Researchers have attempted to quantify the role of turbulence in stream channel erosion by incorporating measures of turbulence into estimations of boundary shear stress (Kim *et al.*, 2000; Biron *et al.*, 2004; Daniels and Rhoads, 2004). Reach-averaged boundary shear stress, although commonplace, does not account for the role of turbulence, and methods that incorporate turbulence parameters may be more appropriate in some applications (Hilldale and Papanicolaou, 2001; Biron *et al.*, 2004; Daniels and Rhoads, 2004). Hilldale and Papanicolaou (2001) assert that conditions for bank erosion are under-predicted by the commonplace critical boundary shear stress method. In our study, water depths were nearly equivalent in all runs (Table I), indicating that reach-averaged boundary shear stress would have been nearly equivalent, as it is a function of the hydraulic radius and energy slope. Various methods of estimating boundary shear stress were tested by Biron *et al.* (2004), and they found that boundary shear stress estimated using TKE produced the best estimate in a complex flow field around deflectors. In the Biron *et al.* (2004) study, patterns of bed scour around deflectors most closely paralleled the distribution of boundary shear stress predicted by a relationship with TKE similar to Equation (4). Daniels and Rhoads (2004) used a similar method to show correlation between boundary shear stress and both the pattern of local bed scour around an LWD obstruction and the widening of a small channel downstream from LWD.

Our estimates of boundary shear stress in W12 indicated that modeled overbank flows would exceed the critical boundary shear stress of some stream bank materials. Although *in situ* measurements of critical boundary shear stresses along the banks of W12 were not available, measured values of critical boundary shear stresses have been published for bank materials in southwestern Virginia and range from 0 Pa to 21·9 Pa (Wynn and Mostaghimi, 2006). Even the most resistant banks measured in the Wynn and Mostaghimi (2006) study would not be able to withstand the boundary shear stresses of the forested runs projected from our results. Inquiry into expected bank erosion is beyond the scope of this study; however, estimates of boundary shear stress indicate a conducive environment for bank erosion and for the initiation of channel widening.

Results from the quadrant analysis may begin to describe how the flow dynamics could promote erosion of the bank surface. The flow dynamics attributed to scour or sediment entrainment along a stream bed have been more widely investigated, and, commonly, the initiation of sediment movement is attributed to sweeps of fluid (Best, 1993; Biron *et al.*, 1993; Buffin-Belanger and Roy, 1998; Papanicolaou *et al.*, 2001). Sweeps occur when higher than average streamwise velocities are coupled with vertical velocities directed toward the bed ($u' > 0$, $w' < 0$; Best, 1993), and they have been associated with bed scour at channel confluences (Biron *et al.*, 1993) and pebble clusters (Buffin-Belanger and Roy, 1998). We suspect that bank scour might be similarly associated with higher than average streamwise velocities coupled with lateral velocities directed into the bank ($u' > 0$, $v' > 0$; quadrant 1 in Table IV). Our quadrant analysis showed that along the bank face quadrant 1 events were predominant in percentage of time and had a greater mean Reynolds shear stress than quadrants 2 ($u' < 0$, $v' > 0$) or 4 ($u' > 0$, $v' < 0$). Experiments with erodible beds and banks would be needed to demonstrate whether this particular flow characteristic might initiate stream bank erosion.

Finally, our investigation of near-bank turbulence suggests that stream banks might become more susceptible to erosion with the introduction of forested vegetation; however, we cannot make direct conclusions about bank stability as this study did not investigate the resistive forces. Although bank stability depends on many different factors, forest vegetation in small streams is often recognized for strengthening banks and slowing channel migration (Stott, 1997; Parkyn *et al.*, 2003; Allmendinger *et al.*, 2005). Given the results of previous studies, we suspect that the high-turbulence shear layer phenomenon observed in this study is a process that would operate only during overbank floods and only for a finite time period. Intermittent overbank flows in streams where forested riparian vegetation is being recolonized or replanted could promote a shift in channel size from the narrow, non-forested equilibrium to a new, wider equilibrium. Over time, we suspect that the widened stream with mature forested riparian vegetation will reach a dynamic equilibrium because velocities and shear stresses will become reduced with the stream's larger capacity. Other processes may function to maintain mature forested reaches in a wider equilibrium and non-forested reaches in a narrower equilibrium, such as described in the model of Allmendinger *et al.* (2005). Allmendinger *et al.* (2005) found rates of deposition and lateral migration to be higher in non-forested reaches than in forested reaches, and they suggest that equilibrium widths develop to equalize rates of cutbank erosion and vegetation-mediated rates of deposition on active floodplains.

Future work

Our results put forth an unacknowledged potential mechanism for channel widening in response to reforestation of riparian areas; however, many aspects of the channel widening phenomenon remain unresolved. Of all the theorized driving mechanisms, we do not know which are significant or how they might interact. Next steps for experimental work might include testing with erodible beds and banks to investigate whether boundary shear stress based on TKE is an appropriate estimation, to explore how bank morphology might respond and interact with the turbulent flow field and to examine whether forested channels might reach an equilibrium size. Moreover, field-based studies are needed to confirm whether experimental results are valid in real streams and to further explore the complexities that cannot be duplicated in a flume experiment, such as seasonal effects, unsteady flow regimes and other natural conditions.

Conclusion

Results of a series of flume experiments simulating stream reaches in transition from non-forested to forested riparian vegetation showed that turbulence generation during overbank flow events may be exacerbated when forested riparian vegetation is introduced. Our flume experiment was a first step to identify the turbulence patterns in overbank flows, with the marked simplification of a fixed bed. Because enhanced turbulence along the bank interface creates instantaneous forces much greater than time-averaged values, boundary shear stresses capable of entraining and transporting sediment are likely amplified. Estimations of boundary shear stress based on TKE illustrated that modeled flows would likely exceed the critical boundary shear stress of some bank materials. Other results such as the location of high turbulence, the spatial extent of the turbulence and patterns in Reynolds shear stresses in forested runs illustrated additional facets of the hydraulic conditions that could initiate bank erosion. Results confirm that this potential driving mechanism for channel widening should be added to the set of plausible theories concerning the morphologic differences between forested and non-forested reaches of small streams, while recognizing that further testing of this mechanism and the aforementioned theories is necessary.

Acknowledgements

Research was supported in part by the National Science Foundation Graduate Fellowship Program, a graduate research assistantship from the Vermont Experimental Program to Stimulate Competitive Research (VT EPSCoR, EPS0236976) and a student equipment grant from NortekUSA. We thank Tracy Owen, Andrea Pearce, Floyd Vilmont and Jeff Buzas for their essential help with flume construction, data collection and data analysis. This paper improved substantially thanks to the helpful reviews of Jim Pizzuto and an anonymous reviewer.

References

Albers J. 2000. *Hands on the Land: A History of the Vermont Landscape*. MIT Press: Cambridge, MA.

Allmendinger NE, Pizzuto JE, Potter N, Johnson TE, Hession WC. 2005. Riparian vegetation and width adjustment in laterally migrating rivers of eastern Pennsylvania, U.S.A. *Geological Society of America Bulletin* **117**: 229–243.

Anderson RJ, Bledsoe BP, Hession WC. 2004. Stream and river channel width response to riparian vegetation, bank material texture, and other factors. *Journal of the American Water Resources Association* **40**: 1159–1172.

Bennett SJ, Alonso CV. 2003. Physically modeling stream channel adjustment to woody riparian vegetation. *EOS Transactions AGU* **84**: Abstract H52A-1171.

Best JL. 1993. On the interactions between turbulent flow structure, sediment transport and bedform development: some considerations from recent experimental research. In *Turbulence: Perspectives on Flow and Sediment Transport*, Clifford NJ, French JR, Hardisty J (eds). Wiley: Chichester; 61–92.

DOI: 10.1002/esp

Biron PM, De Serres B, Roy AG, Best JL. 1993. Shear layer turbulence at an unequal depth channel confluence. In *Turbulence: Perspectives on Flow and Sediment Transport*, Clifford NJ, French JR, Hardisty J (eds). Wiley: Chichester; 197–214.

Biron PM, Robson C, Lapointe MF, Gaskin SJ. 2004. Comparing different methods of bed shear stress estimates in simple and complex flow fields. *Earth Surface Processes and Landforms* **29**: 1403–1415.

Bradshaw P, Ferris DH, Atwell NP. 1967. Calculation of boundary-layer development using the turbulent energy equation. *Journal of Fluid Mechanics* **28**: 593–616.

Buffin-Belanger T, Roy AG. 1998. Effects of a pebble cluster on the turbulent structure of a depth-limited flow in a gravel-bed river. *Geomorphology* **25**: 249–267.

Chanson H. 1999. *The Hydraulics of Open Channel Flow*. Arnold: London.

Charlton FG, Brown PM, Benson RW. 1978. *The Hydraulic Geometry of Some Gravel Rivers in Britain: Wallingford, England*. Hydraulics Research Station: Wallingford, UK.

Clifford NJ, French JR. 1993. Monitoring and modelling turbulent flows: historical and contemporary perspectives. In *Turbulence: Perspectives on Flow and Sediment Transport*, Clifford NJ, French JR, Hardisty J (eds). Wiley: Chichester; 1–34.

Daniels MD, Rhoads BL. 2004. Spatial pattern of turbulence kinetic energy and shear stress in a meander bend with large woody debris. In *Riparian Vegetation and Fluvial Geomorphology*, Bennett SJ, Simon A (eds). American Geophysical Union: Washington, DC; 87–98.

Darby SE. 1999. Effect of riparian vegetation on flow resistance and flood potential. *Journal of Hydraulic Engineering – ASCE* **125**: 443–454.

Davies-Colley RJ. 1997. Stream channels are narrower in pasture than in forest. *New Zealand Journal of Marine and Freshwater Research* **31**: 599–608.

Garcia MH, Lopez F, Dunn C, Alonso CV. 2004. Flow, turbulence, and resistance in a flume with simulated vegetation. In *Riparian Vegetation and Fluvial Geomorphology*, Bennett SJ, Simon A (eds). American Geophysical Union: Washington, DC; 11–28.

Gran K, Paola C. 2001. Riparian vegetation controls on braided stream dynamics. *Water Resources Research* **37**: 3275–3283.

Gregory KJ, Gurnell AM. 1988. Vegetation and river channel form and process. In *Biogeomorphology*, Viles HA (ed.). Blackwell: Oxford; 11–42.

Gregory SV, Swanson FJ, McKee WA, Cummins KW. 1991. An ecosystem perspective of riparian zones: focus on links between land and water. *Bioscience* **41**: 540–551.

Hession WC. 2001. Riparian forest and urban hydrology influences on stream channel morphology: implications for restoration. In *World Water and Environmental Resources Congress*, Phelps D, Sehlke G (eds). American Society of Civil Engineers: Reston, VA.

Hession WC, Johnson TE, Charles DF, Hart DD, Horwitz RJ, Kreeger DA, Pizzuto JE, Velinsky DJ, Newbold JD, Cianfrani C, Clason T, Compton AM, Coulter N, Fuselier L, Marshall BD, Reed J. 2000. Ecological benefits of riparian reforestation in urban watersheds: study design and preliminary results. *Environmental Monitoring and Assessment* **63**: 211–222.

Hession WC, Pizzuto JE, Johnson TE, Horwitz RJ. 2003. Influence of bank vegetation on channel morphology in rural and urban watersheds. *Geology* **31**: 147–150.

Hey RD, Thorne CR. 1986. Stable channels with mobile gravel beds. *Journal of Hydraulic Engineering* **112**: 671–689.

Hilldale R, Papanicolaou A. 2001. Characteristics of flow and erosion in a natural stream with loess-type banks. In *Proceedings of the Federal Interagency Sedimentation Conferences, 1947 to 2001*. US Subcommittee on Sedimentation: Reno, NV; I-176–I-183.

Ikeda S, Kanazawa M. 1996. Three-dimensional organized vortices above flexible water plants. *Journal of Hydraulic Engineering* **122**: 634–640.

JMP. 2002. *JMP Statistics and Graphics Guide*. SAS Institute: Cary, NC.

Johnson CG, Laraway GA. 1971. *Flood Magnitude and Frequency of Small Massachusetts Streams*. USGS: Washington, DC.

Kim SC, Friedrichs CT, Maa JPY, Wright LD. 2000. Estimating bottom stress in tidal boundary layer from acoustic Doppler velocimeter data. *Journal of Hydraulic Engineering – ASCE* **126**: 399–406.

Lane SN, Biron PM, Bradbrook KF, Butler JB, Chandler JH, Crowell MD, McLelland SJ, Richards KS, Roy AG. 1998. Three-dimensional measurement of river channel flow processes using acoustic Doppler velocimetry. *Earth Surface Processes and Landforms* **23**: 1247–1267.

Lu SS, Willmarth WW. 1973. Measurement of the structure of the Reynolds stress in a turbulent boundary layer. *Journal of Fluid Mechanics* **60**: 481–511.

McBride M, Hession WC, Thompson DM. 2005. Riparian vegetation influence on channel widths of small streams: revisiting Sleepers River. In *Managing Watersheds for Human and Natural Impacts*, Moglen GE (ed.). American Society of Civil Engineers: Williamsburg, VA.

McClelland SJ, Ashworth PJ, Best JL. 1996. The origin and downstream development of coherent flow structures at channel junctions. In *Coherent Flow Structures in Open Channels*, Ashworth PJ, Bennett SJ, Best JL, McClelland SJ (eds). Wiley: Chichester; 459–489.

McLean SR, Nelson JM, Wolfe SR. 1994. Turbulence structure over 2-dimensional bed forms – implications for sediment transport. *Journal of Geophysical Research – Oceans* **99**: 12 729–12 747.

Murgatroyd AL, Ternan JL. 1983. The impact of afforestation on stream bank erosion and channel form. *Earth Surface Processes and Landforms* **8**: 357–369.

Naot D, Nezu I, Nakagawa H. 1996. Hydrodynamic behavior of partly vegetated open channels. *Journal of Hydraulic Engineering – ASCE* **122**: 625–633.

Nelson JM, McLean SR, Wolfe SR. 1993. Mean flow and turbulence fields over 2-dimensional bed forms. *Water Resources Research* **29**: 3935–3953.

Nezu I. 2005. Open-channel flow turbulence and its research prospect in the 21st century. *Journal of Hydraulic Engineering – ASCE* **131**: 229–246.

DOI: 10.1002/esp

Nezu I, Onitsuka K. 2001. Turbulent structures in partly vegetated open-channel flows with LDA and PIV measurements. *Journal of Hydraulic Research* **39**: 629–642.

Papanicolaou AN, Diplas P, Dancey CL, Balakrishnan M. 2001. Surface roughness effects in near-bed turbulence: implications to sediment entrainment. *Journal of Engineering Mechanics* **127**: 211–218.

Parkyn SM, Davies-Colley RJ, Halliday NJ, Costley KJ, Croker GF. 2003. Planted riparian buffer zones in New Zealand: do they live up to expectations? *Restoration Ecology* **11**: 436–447.

Pasche E, Rouve G. 1985. Overbank flow with vegetatively roughened flood plains. *Journal of Hydraulic Engineering – ASCE* **111**: 1262–1278.

Rosgen D. 1996. *Applied River Morphology*. Wildland Hydrology: Pagosa Springs, CO.

Roy AG, Biron PM, Buffin-Belanger T, Levasseur M. 1999. Combined visual and quantitative techniques in the study of natural turbulent flows. *Water Resources Research* **35**: 871–877.

Shiono K, Knight DW. 1991. Turbulent open-channel flows with variable depth across the channel. *Journal of Fluid Mechanics* **222**: 617–646.

Smith CR. 1996. Coherent flow structures in smooth-wall turbulent boundary layers: facts, mechanisms, and speculation. In *Coherent Flow Structures in Open Channels*, Ashworth PJ, Bennett SJ, Best JL, McClelland SJ (eds). Wiley: Chichester; 1–39.

Stott T. 1997. A comparison of stream bank erosion processes on forested and moorland streams in the Balquhidder Catchments, Central Scotland. *Earth Surface Processes and Landforms* **22**: 383–399.

Sweeney BW. 1992. Streamside forests and the physical, chemical, and trophic characteristics of piedmont streams in eastern North America. *Water Science and Technology* **26**: 2653–2673.

Sweeney BW, Bott TL, Jackson JK, Kaplan LA, Newbold JD, Stanley LJ, Hession WC, Horwitz RJ. 2004. Riparian deforestation, stream narrowing, and loss of stream ecosystem services. *Proceeding of the National Academy of Sciences* **101**: 14132–14137.

Tennekes H, Lumley JL. 1994. *A First Course in Turbulence*. MIT Press: Cambridge, MA.

Thompson DM. 2004. The influence of pool length on local turbulence production and energy slope: a flume experiment. *Earth Surface Processes and Landforms* **29**: 1341–1358.

Thompson DM. 2007. Turbulence characteristics in a shear zone downstream of a channel constriction in a coarse-grained pool. *Geomorphology* **83**: 199–214.

Thompson D, Wohl E. 1998. Flume experimentation and simulation of bedrock channel processes. In *Rivers over Rock: Fluvial Processes in Bedrock Channels*, Tinkler KJ, Wohl EE (eds). American Geophysical Union: Washington, DC; 279–296.

Tinkler KJ. 1997. Critical flow in rockbed streams with estimated values for Manning's *n*. *Geomorphology* **20**: 147–164.

Trimble SW. 1997. Stream channel erosion and change resulting from riparian forests. *Geology* **25**: 467–469.

Trimble SW. 2004. Effects of riparian vegetation on stream channel stability and sediment budgets. In *Riparian Vegetation and Fluvial Geomorphology*, Bennett SJ, Simon A (eds). American Geophysical Union: Washington, DC; 153–170.

Tritton DJ. 1988. *Physical Fluid Dynamics*. Clarendon: Oxford.

Tsujimoto T. 1996. Coherent fluctuations in a vegetated zone of open-channel flow: causes of bedload lateral transport and sorting. In *Coherent Flow Structures in Open Channels*, Ashworth PJ, Bennett SJ, Best JL, McClelland SJ (eds). Wiley: Chichester; 375–396.

Vermont Agency of Transportation (VTAOT). 1998. *Hydraulics Manual*. Vermont Agency of Transportation: Montpelier, VT.

Wahl TL. 2000. Analyzing ADV data using WinADV. In *Proceedings of the 2000 Joint Conference on Water Resources Engineering and Water Resources Planning and Management*, Hotchkiss RH, Glade M (eds). American Society of Civil Engineers: Minneapolis, MN.

Wormleaton PR. 1996. Floodplain secondary circulation as a mechanism for flow and shear stress redistribution in straight compound channels. In *Coherent Flow Structures in Open Channels*, Ashworth PJ, Bennett SJ, Best JL, McClelland SJ (eds). Wiley: Chichester; 581–608.

Wynn T, Mostaghimi S. 2006. The effects of vegetation and soil type on streambank erosion, southwestern Virginia, USA. *Journal of the American Water Resources Association* **42**: 69–82.

Zar JH. 1999. *Biostatistical Analysis*. Prentice-Hall: Upper Saddle River, NJ.

Zimmerman RC, Goodlett JC, Comer GH. 1967. The influence of vegetation on channel form of small streams. In *Symposium on River Morphology*. International Association of Scientific Hydrology: Bern; 255–275.

DOI: 10.1002/esp